SIMULATION OF LASER - ELECTRON BEAM INTERACTION IN THE OPTICAL KLYSTRON OF A FREE ELECTRON LASER

C.A. Thomas, J.I.M. Botman, Eindhoven University of Technology, The Netherlands,

C.A.J. van der Geer, FOM Institute for Plasma Physics, "Rijnhuizen", The Netherlands,

M.E. Couprie, CEA/SPAM Lure, Orsay, France

Abstract

The particle optics code GPT [1] has been applied to study the single pass electron beam interaction with an external laser field in the undulator system of a free electron laser. In particular, this code has been used to simulate the laser - electron beam interaction in an optical klystron. Micro-bunching as a result of the interaction of the electron bunch with an electromagnetic pulse is presented. The energy exchange during the interaction calculated with GPT gives the gain curve of the optical klystron.

1 INTRODUCTION

Simulations with the General Particle Tracer code [1] (GPT) have been performed, to study the interaction of an electron bunch with an external electromagnetic pulse during one pass through an optical klystron. The simulations show the micro-bunching of the electrons resulting from the interaction electron – electromagnetic pulse. The gain curve of the optical klystron given by the interaction is presented.

2 SIMULATION SET UP FOR GPT

The GPT code is a 3D simulation platform for the study of charged particle dynamics in electromagnetic fields. The code solves the differential equation of motion for each particle, taking into account the electromagnetic field felt by the particle. The results are in a file containing the time evolution of the position, the velocity, the normalized energy of each particle and the electro-magnetic field felt by the particle. The time evolution of the normalized energy gives information about the energy exchange between electrons and the external field during the passage through the optical klystron. We use this simulation code to focus on the interaction of the electron bunch and an electro-magnetic pulse in an optical klystron. In the laboratory frame (x,y,z), were z is the longitudinal axis, x the horizontal bending axis, and y the vertical axis, the electron bunch is defined by the longitudinal and transverse distributions ($<z>$, σ_z), ($<x>$, σ_x) and ($<y>$, σ_y), the energy distribution (E_0, σ_E) and the emittances, (ε_x, ε_y). We assume gaussian distributions (table 1).

The optical klystron, similar to the one of Super ACO [2], is composed of two identical planar undulators, 10 periods

of length λ_0 and a field amplitude B_u, separated by a dispersive section. In the dispersive section the magnetic field has two periods of length λ_d and a field amplitude $B_d > B_u$. The magnetic field of the dispersive section satisfies the conditions to leave the electron trajectories on the same axis in both two undulators [3] (figure 1). The electromagnetic pulse is monochromatic, at the resonance wavelength [4-5] $\lambda_r = \dfrac{\lambda_0}{2\gamma^2}\left(1 + K^2\right)$, where γ is the relativistic factor and K the undulator strength [4], and is first approximated by a plane wave inside the interaction volume $V = \pi \, \sigma_r^2 \, \sigma_l$, where σ_r and σ_l are the transverse and longitudinal size of the electromagnetic pulse. The energy of the pulse is $I = \frac{1}{2} \, \varepsilon_0 \, E^2 \, V$, where E is the amplitude of the electric field.

Table 1: Input parameters for GPT optical klystron simulations.

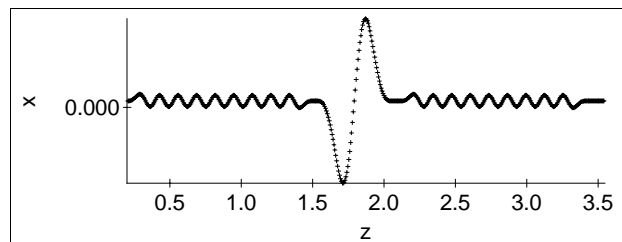| Electron bunch	
Length (σ_z)	30 mm
Radius (σ_x, σ_y)	0.1 mm
energy (E_0)	800 MeV
Relative energy spread (σ_ε)	$9 \cdot 10^{-4}$
Emittances (ε_x, ε_y)	$3. \, 10^{-8}$ m rad
Current (I_b)	30 mA
Optical Klystron	
Period (λ_0)	130 mm
Number of periods (N_u)	10
Strength (K)	3
Dispersive section (N_d)	60
Electromagnetic pulse	
Wavelength (λ_r)	264.8 nm
Length (σ_l)	3 mm
Radius (σ_r)	0.1 mm
Energy (I)	1 μJ to 10 mJ

Figure 1: Electron trajectory in the optical klystron, in the (x,z) plane.

3 SIMULATION RESULTS

In the simulations with GPT, taking the electron bunch as defined in table 1, but restricting the calculation to 10 wavelengths λ_r, and gradually increasing the energy of the electromagnetic pulse, micro bunching in the (x,z) plane becomes visible behind the dispersive section above the value 5 µJ (figure 2).The micro-bunching process appears as the result of the exchange of energy between the electrons and the electro-magnetic pulse which leads to redistribute the electron longitudinal positions in the bunch. The action of the dispersive section can be observed as a rotation in the longitudinal phase space (figure 4). At very high energy, $I > 0.1$ mJ, the micro-bunching appears in the first undulator and the micro-bunches are spread by the dispersive section in the second undulator (figure 3). Saturation [5] takes place and the energy exchange is limited, as will be shown at the end of the section.
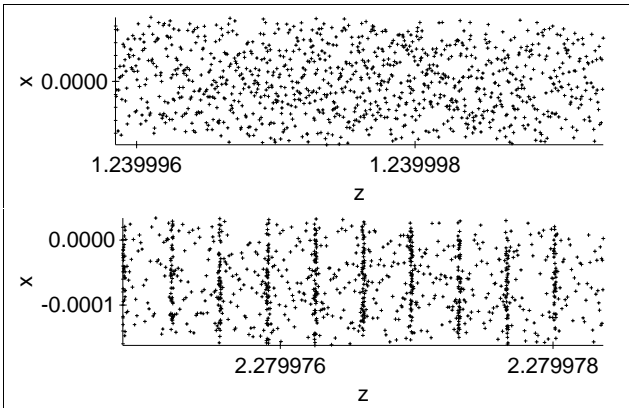

Figure 2: Part of the bunch. The micro-bunches appear behind the dispersive section and are separated by the ponderomotive wavelength. I=10 µJ.
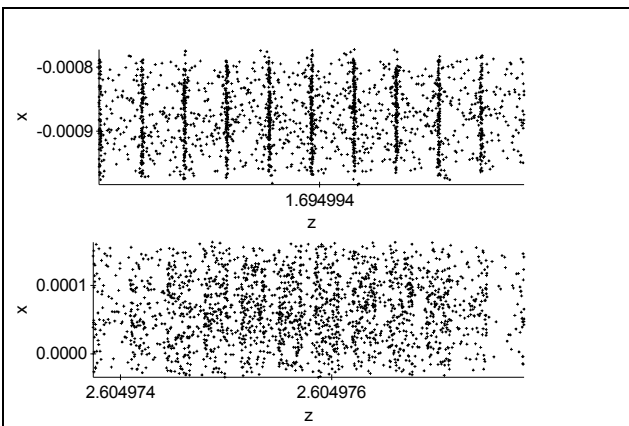

Figure 3: Part of the bunch at saturation. The micro-bunching appears in the first part of the optical klystron and is spread in the second part. I=10 mJ.

The phase plane (z, β_z), where β_z is v_z/c (c and v_z are respectively the light and electron longitudinal velocity), shows the same behavior of the bunch. When $I > 5$ µJ, a substantial part of the electrons start to be trapped in the potential well of the ponderomotive wave after the dispersive section (figure 4). When $I > 0.1$ mJ, all the electrons are trapped in the second part of the optical klystron (figure 5).
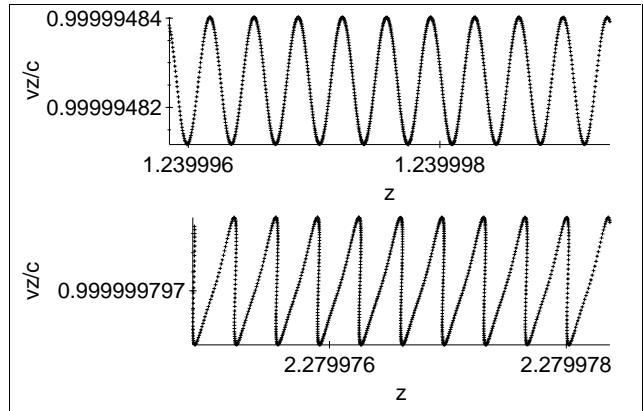

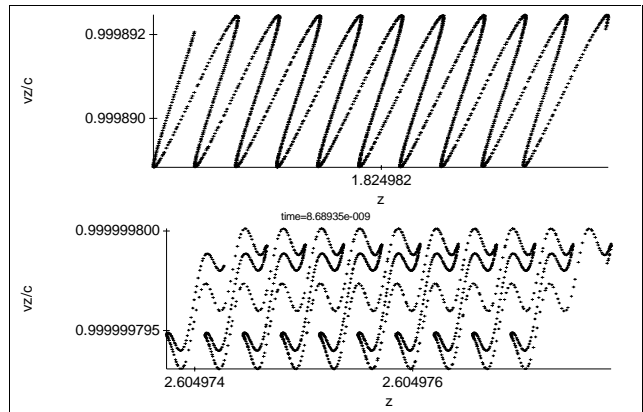Figure 4: Part of the bunch in phase space (z,β_z). I=10 µJ.

Figure 5: Part of the bunch in phase space (z, β_z). I=10 mJ.

Although GPT offers the possibility to include complete particle wave interaction we have chosen here for the simpler approach, to use the energy exchange $\Delta\gamma$ between the electron bunch and the electromagnetic pulse to calculate the gain. This approximation is valid as long as the wave amplitude changes only little during a simulation, which is the case for the low gain regime. For practical reasons, the frequency dependence of the gain is determined by repeating the simulation for different initial energies of the mono-energetic bunch E_b, around the resonance energy E_0. The curve obtained, $\Delta\gamma$ vs. E_b, is proportional to the gain curve [6]. The gain curve as expected is proportional to the derivative of the spontaneous emission of the optical klystron (figure 6).

The gain curve obtained has been fit with the expression [7]

$$G = g_0 \sin c(\delta) \sin\left(2\pi\left(N + N_d\right)\frac{\lambda_r}{\lambda}\right),$$

and $\delta = \pi N_u\left(1 - \frac{\lambda_r}{\lambda}\right)$, where N_d is the order of interference determined by the dispersive section [6].

The parameters of the fitting curve are the same as in the simulations.
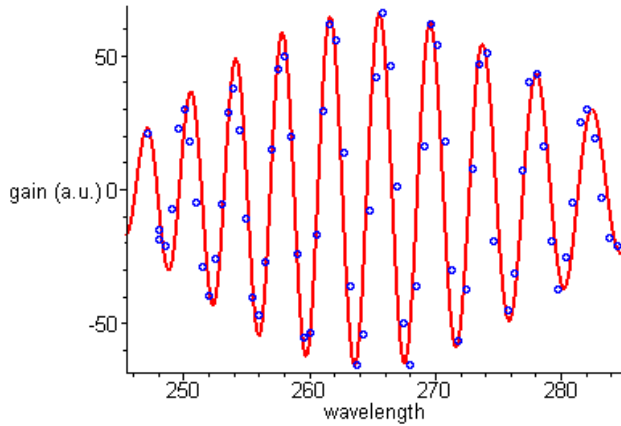

Figure 6: The gain curve of the optical klystron. The curve fits the derivative of the spontaneous emission. The parameters of the fitting curve are $\lambda_r = 265$ nm, $N_u = 10$, $N_d = 57$, i.e. the same parameters as those used for the simulation.

Taking the same bunch with the energy corresponding to the maximum energy loss, i.e. the maximum gain, and increasing the energy of the electromagnetic pulse from 1 µJ to 10 mJ, the energy exchange is maximum in the range 10 to 100 µJ (table 2). Calculating the saturation energy [8] gives the value $I_{sat} = 50$ µJ. When I is larger than I_{sat} the spreading of the micro-bunching in the second part of the optical klystron, which was maximum in the first part, indicates electrons re-absorb energy from the electromagnetic pulse. This process leads to the saturation of the gain. We note that this saturation process does not correspond to that of an SRFEL, but to a single pass FEL where the electron bunch has a definite and constant energy spread at the entrance of the optical klystron.

Table 2: Average energy loss, $\Delta\gamma$ vs. I.

I (µJ)	1	10	100	10^3	10^4
$-\Delta\gamma$	0.006	0.054	0.442	0.272	0.152

Looking at the energy distribution, one can observe the usual coherent modulation [5] of the electron energy in the optical klystron (figure 7). At the entrance of the optical klystron the energy distribution is gaussian (truncated). At the end, the effect of the electromagnetic pulse is to induce a coherent modulation of the electron's energy.
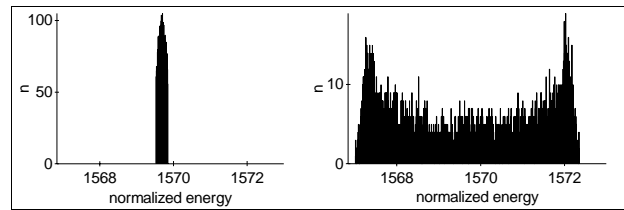

Figure 7: Normalized energy distribution (γ) of the bunch before the entrance and at the end of the optical klystron. $I = 10$ µJ

4 CONCLUSION AND FUTURE WORK

The results that have been obtained with GPT describe a single pass of an electron bunch in an optical klystron with a given external field. Micro-bunching, exchange of energy between electrons and a monochromatic light pulse, and saturation effects can be seen. These results are in agreement with the single-mode low-gain theoretical results. The model will be extended in order to study the dynamics of the SRFEL. This extension requires inclusion of the rest of the storage ring, albeit in a simplified way, and multi-pass simulation. This will require complete particle-wave interaction to be taken into account, as the light amplitude will change over a large range. It will be necessary to equip GPT with a complete set of longitudinal modes of an optical cavity, covering the range [λ_{min}, λ_{max}] of wavelengths defined by the gain curve. This will provide the possibility to follow the evolution of the longitudinal profile of the radiation from the starting point, from spontaneous emission to saturation.

REFERENCES

[1] General Particle Tracer: A new 3D code for accelerator and beamline design, M.J. de Loos, S.B. van der Geer, Proc. 5th Eur. Part. Acc. Conf., Sitges, (1996)pp. 1241.

[2] Super ACO FEL oscillation at 300nm, D. Nutarelli et al. Nucl. Instr. and Meth. A 445 (2000) 143-148.

[3] Free Electron Laser Undulators, Electron Trajectories and Spontaneous Emission, P. Elleaume, *Laser Handbook Vol. 6, edited by W.B. Colson, C. Pelligrini and A. Renieri.*

[4] Classical Free Electron Laser Theory, W.B. Colson, *Laser Handbook Vol. 6, edited by W.B. Colson, C. Pelligrini and A. Renieri.*

[5] Experimental and Theoretical Aspects of the Free Electron Laser, G. Dattoli and A. Renieri, *Laser Handbook Vol 4, edited by M.L. Stitch and M. Bass.*

[6] Felix Design and Instrumentation, C.A.J. van der Geer, Thesis Eindhoven Technological University (1999).

[7] Laser à Electron Libres sur anneau de stockage, M.E. Couprie, Thèse de doctorat de l'Université Paris Sud (1989)

[8] Lectures on the Free Electron Laser Theory and related topics, G. Dattoli, A. Renieri, A. Torre, *World Scientific* (93), p570.